OPEN

Morphologic, Immunohistochemical, and Genetic Differences Between High-grade and Low-grade Fetal Adenocarcinomas of the Lung

Yue Li, MD,† Shao-yan Xi, MD,*‡ Juan-juan Yong, MD,§ Xiao-yan Wu, MM,*† Xin-hua Yang, MM,*† and Fang Wang, MD*†*

Abstract: Fetal adenocarcinoma of the lung (FLAC) is a rare lung tumor classified into low-grade fetal adenocarcinoma of the lung (LG-FLAC) and high-grade fetal adenocarcinoma of the lung (HG-FLAC). It remains debatable whether HG-FLAC is a subset of FLAC or a distinct subtype of the conventional lung adenocarcinoma (CLA). In this study, samples of 4 LG-FLAC and 2 HG-FLAC cases were examined, and the clinicopathologic, immunohistochemical (IHC), and mutational differences between the 2 subtypes were analyzed using literature review. Morphologically, LG-FLACs had a pure pattern with complex glandular architecture composed of cells with subnuclear and supranuclear vacuoles, mimicking a developing fetal lung. In contrast, HG-FLACs contained both fetal lung-like (FLL) and CLA components. With regard to IHC markers, β-catenin exhibited a nuclear/cytoplasmic staining pattern in LG-FLACs but a membranous staining pattern in HG-FLACs. Furthermore, p53 was expressed diffusely and strongly in HG-FLACs, whereas in LG-FLACs, p53 staining was completely absent. Using next-generation sequencing targeting a 1021-gene panel, mutations of *CTNNB1* and *DICER1* were detected in all 4 LG-FLAC samples, and a novel mutation, *MYCN* P44L, was discovered in 2 LG-FLAC samples. DNA samples of the FLL and CLA components of HG-FLACs were separately extracted and sequenced. The FLL component harbored no *CTNNB1*, *DICER1*, or *MYCN* mutations; moreover, the FLL genetic profile largely overlapped with that of the CLA component. The morphologic, IHC, and genetic features of HG-FLAC indicate that it is a variant of CLA rather than a subset of FLAC. Thus, HG-FLAC should be treated differently from LG-FLAC.

Key Words: fetal adenocarcinoma of the lung, *CTNNB1 DICER1*, *MYCN*, mutational profile

(*Am J Surg Pathol* 2021;45:1464–1475)

Fetal adenocarcinoma of the lung (FLAC) is a rare malignant lung tumor, accounting for 0.1% to 0.5% of all pulmonary neoplasms.[1] It was reported as a subtype of pleuropulmonary blastoma lacking a sarcomatous component in 1982,[2] and the term "well differentiated fetal adenocarcinoma of the lung" was introduced afterwards.[3] As the name implies, FLAC morphologically resembles a developing fetal lung during the pseudoglandular phase: complex glandular components with tubules are lined by glycogen-rich, nonciliated cells.[4] In the World Health Organization classification of 2015, FLAC was further classified into low-grade fetal adenocarcinoma of the lung (LG-FLAC) and high-grade fetal adenocarcinoma of the lung (HG-FLAC) based on their different clinicopathologic features.[5] LG-FLAC has a pure pattern, displaying mild nuclear atypia and typical morule formation. In contrast, HG-FLAC is generally composed of both fetal lung-like (FLL) and conventional lung adenocarcinoma (CLA) components, such as acinar type, papillary type, micropapillary type, lepidic type, and solid type, with prominent nuclear atypia, necrosis, and pathologic mitoses. LG-FLAC tends to occur in young female nonsmokers, with a peak incidence in the fourth decade of life, whereas HG-FLAC occurs more frequently in elderly male smokers.[6]

It remains inconclusive whether HG-FLAC is a subset of FLAC with a higher grade or merely a distinct

From the *State Key Laboratory of Oncology in South China, Collaborative Innovation Center for Cancer Medicine; Departments of †Molecular Diagnostics; ‡Pathology, Sun Yat-Sen University Cancer Center; and §Department of Pathology, Sun Yat-Sen Memorial Hospital, Sun Yat-Sen University, Guangzhou, People's Republic of China.

Y.L. and S.-y.X. contributed equally.

Funded by the Guangdong Basic and Applied Basic Research Foundation (grants 2020A1515010314 and 2020A1515010098), the National Natural Science Foundation of China (grant 82002561), the Natural Science Foundation of Guangdong Province (grant 2017A030310192), and the Fundamental Research Funds for the Central Universities (grant 17ykpy84).

Conflicts of Interest and Source of Funding: The authors have disclosed that they have no significant relationships with, or financial interest in, any commercial companies pertaining to this article.

Correspondence: Fang Wang, MD, No. 651, Dongfeng East Road, Yuexiu District, Guangzhou 510060, People's Republic of China (e-mail: wangfang@sysucc.org.cn).

Supplemental Digital Content is available for this article. Direct URL citations appear in the printed text and are provided in the HTML and PDF versions of this article on the journal's website, www.ajsp.com.

Copyright © 2021 The Author(s). Published by Wolters Kluwer Health, Inc. This is an open access article distributed under the terms of the Creative Commons Attribution-Non Commercial-No Derivatives License 4.0 (CCBY-NC-ND), where it is permissible to download and share the work provided it is properly cited. The work cannot be changed in any way or used commercially without permission from the journal.

subtype of CLA. It has been previously reported that epithelial cells of HG-FLAC display membranous β-catenin staining, whereas LG-FLAC cells express β-catenin in an aberrant nuclear/cytoplasmic pattern.[4,6] It has been suggested that >90% of LG-FLACs harbor neuroendocrine cells expressing chromogranin A (CgA) and/or synaptophysin (Syn), whereas only about 50% of HG-FLACs contain such cells.[6,7] Mutations of *CTNNB1* are considered as a characteristic signature of LG-FLAC, but they are seldom observed in HG-FLAC.[4,8] Recently, LG-FLAC was reported as one of the manifestations of *DICER1* syndrome, a pleiotropic tumor predisposition syndrome associated with an increased risk of malignant and nonmalignant neoplasms.[9] However, *DICER1* mutations have not been reported in HG-FLAC cases. Accumulating evidence indicates differences between HG-FLAC and LG-FLAC, so the question of their similarity requires a comprehensive analysis.

Molecular analysis is a very useful tool to describe and diagnose a disease from the genetic point of view.[10] However, genetic testing used to be limited to panels with small numbers of genes in the past.[4,8] In the current study, molecular analysis was conducted using the next-generation sequencing (NGS) approach covering 1021 genes, and the FLL and CLA components of HG-FLAC tissue samples were separately macrodissected and sequenced. By performing a full-scale analysis of the clinicopathologic, immunohistochemical (IHC), and genetic features of 4 cases of LG-FLAC and 2 cases of HG-FLAC, we sought to improve the categorization of HG-FLAC and establish new genetic markers for the differential diagnosis of LG-FLAC.

MATERIALS AND METHODS

Clinical Samples

FLAC cases were retrospectively screened by searching the electronic pathologic records in the Sun Yat-sen University Cancer Center and the Sun Yat-sen Memorial Hospital between January 2013 and December 2020. Clinical information, such as sex, age, chief complaint, smoking history, treatment, and follow-up, was obtained from the medical records of inpatient or outpatient visits, as well as from telephone interviews until February 25, 2021. The TNM stage was evaluated as per the 8th Union for International Cancer Control TNM staging system for non−small cell lung cancer (NSCLC). Overall survival (OS) was calculated as the duration from the date of diagnosis to the date of death from any cause or to the last follow-up. The use of human tissue samples and clinical data was approved by the Ethics Committees of the Sun Yat-Sen University Cancer Center (B2020-344-01). All patients provided signed informed consent, and the research was carried out in accordance with the Declaration of Helsinki.

In addition, papers published in English were searched using key words such as "well-differentiated/low-grade," "high-grade," "fetal adenocarcinoma of the lung," "fetal pulmonary adenocarcinoma" and their combinations in PubMed (www.ncbi.nlm.nih.gov/pubmed/). Published reports with detailed clinicopathologic description and/or featured molecular findings were summarized together with the data from the present study.

Pathologic Diagnosis and IHC

The pathologic diagnoses of FLAC were reconfirmed by independent consultations with 2 experienced pathologists (S-.y.X. and J-.j.Y.) according to the World Health Organization 2015 criteria.[5] IHC experiments were conducted using a BenchMark XT automated immunostainer (Ventana, Tucson, AZ) along with the appropriate positive and negative controls. The primary antibodies are listed in Table 1. A sample was considered as IHC-positive when moderate-to-strong staining was observed in ≥10% of the tumor cells. All IHC staining slides were reviewed by 2 experienced pathologists (S-.y.X. and J-.j.Y.). Whole slide images were generated using the digital slide scanner KF-PRO-005-EX (KFBIO, Ningbo, China), and all microphotographs were exported by reading whole slide images with K-ViEWER version 1.5.3.1 (KFBIO).

Tissue Macrodissection and DNA Isolation

The tumorous and patient-matched normal lymph node tissue sections were cut into 4 to 5-μm-thick sections, and the regions containing >70% of tumor cells on unstained sections were selectively macrodissected according to the hematoxylin and eosin (H&E) staining. For each HG-FLAC sample, the contours of the FLL and CLA regions were marked on the H&E slide under a microscope, and the 2 different morphologic components were

TABLE 1. The Information of IHC Primary Antibodies

Antibodies	Clone	Type	Source	Dilution	Staining Pattern
TTF-1	SP141	Rabbit, mono	Ventana	RTU	N
β-Catenin	UMAB15	Mouse, mono	Ventana	1:300	M, C/N
p53	DO7	Mouse, mono	Ventana	1:400	N
SALL-4	6E3	Mouse, mono	Ventana	1:50	N
Syn	SP11	Rabbit, mono	Ventana	1:100	C
CgA	EP38	Rabbit, mono	Ventana	1:400	C
Gly-3	1G12	Mouse, mono	Ventana	1:100	C/M
AFP	EP209	Rabbit, mono	Ventana	1:150	C

C/M indicates cytoplasmic/membranous staining; C/N, cytoplasmic/nuclear staining; Gly-3, glypican-3; M, membranous staining; RTU, ready-to-use; TTF-1, thyroid transcription factor-1.

Copyright © 2021 The Author(s). Published by Wolters Kluwer Health, Inc.

macrodissected according to their respective contours, so that corresponding DNA could be separately isolated and sequenced. The genomic DNA was extracted using a QIAamp DNA FFPE Tissue kit (Qiagen, Hilden, Germany) and then quantified with a Qubit Fluorometer using the Qubit dsDNA BR assay (Life Technologies, Carlsbad, CA).

NGS and Data Processing

NGS was performed by Geneplus Ltd (Beijing, China). Methods for sequencing library preparation and data analysis were described previously.[11,12] Briefly, fragmented DNA (1.0 g) was mixed with Illumina-indexed adapters for library construction using a KAPA Library Preparation Kit (Kapa Biosystems, Wilmington, MA). Custom-designed probes covering about 1.1 Mb of genomic sequences of 1021 cancer-related genes were used for DNA capture. Sequencing was performed on a Geneplus 2000 Sequencing System (Beijing, China) with 2×100 bp paired-end reads. Matched normal lymph node tissue samples were sequenced as control to filter germline variation. The data was processed as previously described[13–16] and detailed in the Supplementary Methods (Supplemental Digital Content 2, http://links.lww.com/PAS/B187).

RESULTS

Clinical Characteristics

Detailed clinical information about each patient is presented in Table 2. One patient with LG-FLAC was female, the others were males. The average ages of the LG-FLAC and HG-FLAC groups were 37.3 (30 to 48) and 50.5 (39 to 62) years, respectively. Both patients with HG-FLAC were heavy smokers. Patient HG1 consumed 1 pack of cigarettes per day for about 40 years, and he had a 40-year drinking history. Patient HG2 smoked 1 pack of cigarettes every day for 15 years. In contrast, all 4 LG-FLAC patients were nonsmokers. The chief complaints included fever, cough, sputum, and hemoptysis. Two patients with LG-FLAC had no symptoms, and lung nodules were found accidentally during a regular physical examination. One LG-FLAC patient and 1 HG-FLAC patient were diagnosed at stage IVB, whereas the others were

TABLE 2. Clinical Information of Patients With LG-FLAC and HG-FLAC in the Present Study and Literature Review

References	Diagnosis	Sex	Age (y)	Chief Complaint	Smoking	TNM	Treatment	Follow-up (mo)
This study	LG-FLAC	Male	30	Pulmonary nodule	Nonsmoker	pT1bN0M0, IA	Lobectomy and mediastinal lymphadenectomy	99.5, NED
This study	LG-FLAC	Male	36	Fever, cough, blood in phlegm	Nonsmoker	pT2aN0M0, IB	Lobectomy and mediastinal lymphadenectomy+post-operative chemotherapy	36.4, NED
This study	LG-FLAC	Male	48	Pulmonary nodule	Nonsmoker	pT3N0M0, IIB	Left total pneumonectomy and mediastinal lymphadenectomy	26.4, NED
This study	LG-FLAC	Female	35	Cough	Nonsmoker	pT2aN2M1c, IVB	Palliative chemotherapy	3.8, NED
This study	HG-FLAC	Male	62	Cough, sputum and hemoptysis	40 p-y	pT2bN0M0, IIA	Lobectomy and mediastinal lymphadenectomy+post-operative chemotherapy	32.7, NED
This study	HG-FLAC	Male	39	Cough and blood in phlegm	15 p-y	pT4N0M1c, IVB	Neoadjuvant chemotherapy +lobectomy and mediastinal lymphadenectomy+post-operative chemotherapy	13.7, DOD
Sato et al[17]	LG-FLAC	10 male/ 15 female	Mean, 37	19/25 asymptomatic	ND	22 I/1 II/1 IV/ 1 ND	ND	Mean, 39; 20 NED/2 DOD/3 ND
Morita et al[7]	HG-FLAC	16 male/ 1 female	Median, 64.2	Cough or chest pain	Median, 54.9 p-y	7 I/6 II/4 III	Lobectomy and standard lymph node dissection	Median, 29.3; 5 y OS 53.6%
Suzuki et al[18]	HG-FLAC	14 male/ 6 female	Median, 67.3	ND	10/20 smokers, median 50 p-y	7 I/5 II/6 III/2 IV	ND	Mean, 34.9; 5 y OS 82.4%
Zhang et al[4]	HG-FLAC	4 male/ 1 female	Mean, 60.4	ND	4/5 smokers	2 I/3 III	ND	Median, 98; 2 NED/3 DOD
Zhang et al[4]	LG-FLAC	2 male/ 1 female	Mean, 36.3	ND	0/3 smokers	3 I	ND	Median, 10; 3 NED
Suzuki et al[19]	HG-FLAC	43 male/ 10 female	Median, 67	ND	41/53 smokers	29 I/13 II/11 III	Pulmonary lobectomy	Median, 33.1; 5 y OS 49%
Zhang et al[20]	LG-FLAC	23 male/ 22 female	Mean, 35	Cough, blood-streak sputum, chest pain, fever, hemoptysis	12/45 smokers	8 I/21 II/2 III/ 1 IV/13 ND	All underwent surgery, 10/45 also received radiotherapy and/or chemotherapy	Median, 24; 25 NED/5 DOD/1 Relapse/14 ND

DOD indicates died of disease; ND, no description; NED, no evidence of disease; p-y, packs×years.

Copyright © 2021 The Author(s). Published by Wolters Kluwer Health, Inc.

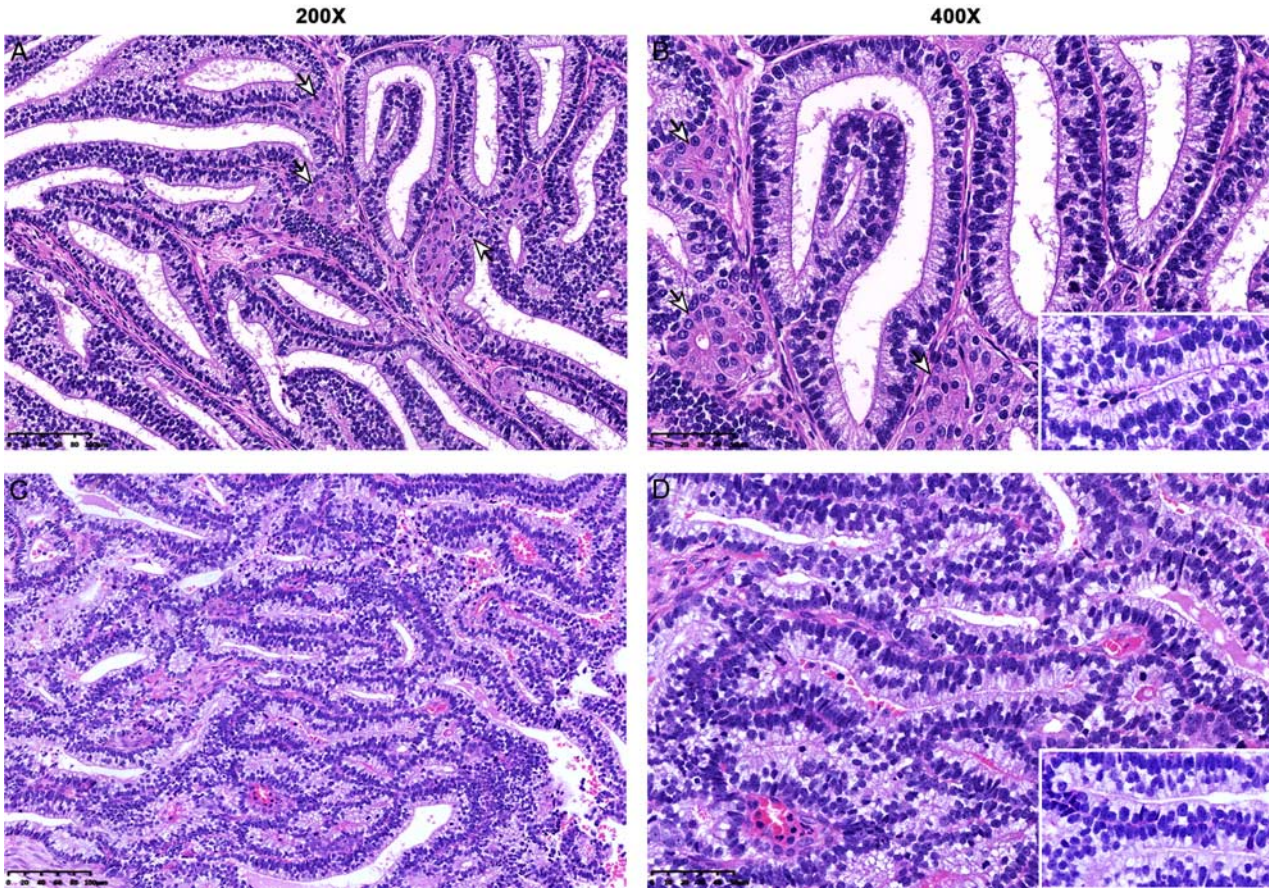

FIGURE 1. Morphologic features of LG-FLAC revealed by H&E staining. A–D, Complex glandular structures resembling the developing fetal lung composed of columnar cells and typical morule foci (A, B, white arrows). Typical glandular cells with supranuclear or subnuclear cytoplasmic vacuolization are demonstrated in the insets (B, D).

diagnosed at stages I to II. The median follow-up duration was 29.6 months (range, 3.8 to 99.5 mo).

Morphologic Features

As can be observed in the H&E slices, LG-FLACs were pure in pattern with quite complex glandular structure. The cells lining the inner side of the glands exhibited relatively low nuclear atypia and presented with subnuclear and supranuclear vacuoles, mimicking an endometrioid appearance, which is a distinguishing mark of LG-FLAC (Figs. 1A–D). Meanwhile, squamoid morules, defined as gathered solid nested squamous epithelial clusters, were found focally in 3 cases of LG-FLAC (white arrows in Figs. 1A, B). Both HG-FLAC cases exhibited a mixture of FLL and CLA morphologies. The tubular glands were formed by densely packed branches lined by glycogen-rich columnar cells with clear cytoplasm, prominent nucleoli, high nuclear atypia, and frequent mitoses. Compared with the morphologic features of LG-FLACs, morule formation was absent, whereas multifocal necrosis was quite frequently observed in both HG-FLAC cases (Figs. 2A–D). A zone of morphologic transition from the FLL component to the CLA acinar pattern could be recognized in one of the HG-FLAC samples (Figs. S1A–D, Supplemental Digital Content 3, http://links.lww.com/PAS/B186). None of the HG-FLAC cases presented with large cell neuroendocrine cells, squamous cells, or small cell differentiation.

IHC Findings

Differential IHC staining features for several markers, including thyroid transcription factor-1, β-catenin, p53, SALL-4, Syn, CgA, alpha-fetoprotein (AFP) and glypican-3, have been reported in HG-FLAC and LG-FLAC.[4,7] We stained samples from all the 6 cases for these markers, and the results are summarized in Table 3. The neoplastic glandular cells of both LG-FLAC and HG-FLAC showed diffused staining for thyroid transcription factor-1 (Figs. 3A, 4A). LG-FLAC cells exhibited clear cytoplasmic and/or nuclear β-catenin staining (Fig. 3B), whereas in HG-FLAC tumor cells, β-catenin was expressed in the cell membranes (Fig. 4B). The p53 protein was expressed diffusely and strongly in HG-FLAC cells but was nearly absent in LG-FLAC cells (Figs. 3C, 4C), which indicated that HG-FLAC is closer to CLA. SALL-4-positive and Syn-positive cells were noted in some areas of LG-FLAC samples, where 0% to 55% of all cells exhibited corresponding staining (Figs. 3D, E). However, such staining barely appeared in

Copyright © 2021 The Author(s). Published by Wolters Kluwer Health, Inc.

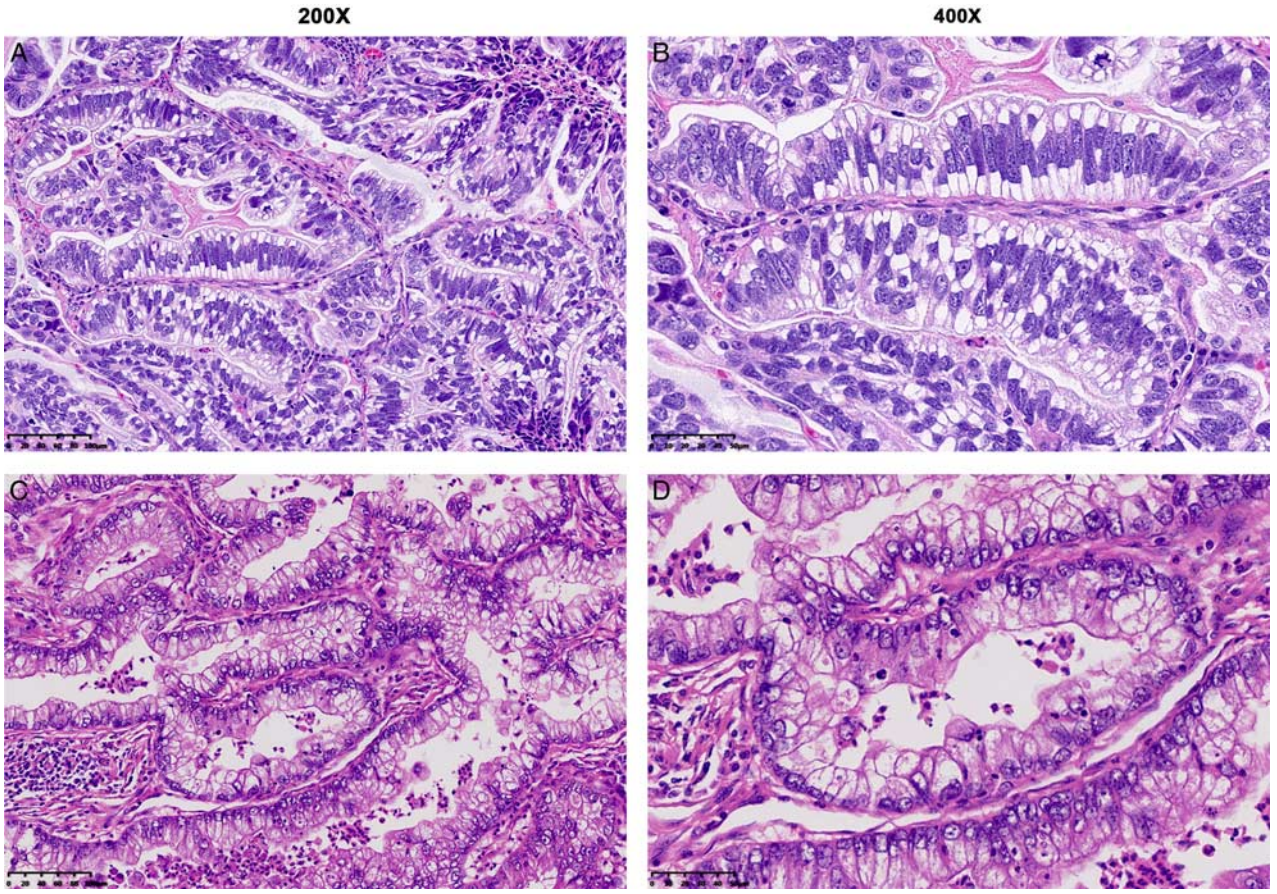

FIGURE 2. Histologic manifestations of HG-FLAC by H&E staining. A–D, Typical FLL morphology of HG-FLACs: glandular cells with supranuclear or subnuclear vacuoles, prominent nuclear atypia, frequent mitoses, and multifocal necrosis.

HG-FLAC specimens (Figs. 4D, E). Both HG-FLAC and LG-FLAC samples were negative for CgA, AFP, or glypican-3 staining (Figs. 3F–H, 4F–H).

Molecular Profiling

To better understand the genetic alterations underpinning HG-FLAC and LG-FLAC, we adopted NGS technology targeting 1021 cancer-related genes to explore molecular profiles of the 2 FLAC subtypes. All 4 LG-FLAC cases had missense mutations in exon 3 of *CTNNB1* (S33C, S37F, D32Y, and S37F, respectively). Two missense mutations (D1709V and D1709A) of *DICER1* were also found in case LG1, 1 deletion mutation (A1710del) and 1 deletion-insertion mutation (D1810F) of *DICER1* were revealed in case LG2, 1 nonsense mutation (Q488*) in *DICER1* was found in case LG3, and 1 splice

TABLE 3. IHC Features of LG-FLAC and HG-FLAC Cases in the Present Study and Literature Review

References	Diagnosis	TTF1	β-Catenin	p53	AFP	SALL-4	Gly-3	CgA	Syn
This study	LG-FLAC	+	C/N+	−	−	−	−	−	−
This study	LG-FLAC	+	C/N+	−	−	+, 30%	−	−	+, 1%
This study	LG-FLAC	+	C/N+	−	−	+, 55%	−	−	−
This study	LG-FLAC	+	C/N+	−	−	+, 40%	−	−	+, 1%
This study	HG-FLAC	+	M+	+, 80%	−	−	−	−	−
This study	HG-FLAC	+	M+	+, 90%	−	−	−	−	−
Sato et al[17]	LG-FLAC	ND	ND	ND	ND	ND	ND	ND	ND
Morita et al[7]	HG-FLAC	+, 7/17	ND	+, 10/17	+, 5/17	+, 9/17	+, 13/17	+, 5/17	+, 6/17
Suzuki et al[18]	HG-FLAC	+, 10/20	ND	ND	+, 19/20	+, 8/20	+, 7/20	+, 9/20	+, 8/20
Zhang et al[4]	HG-FLAC	+, 1/5	M+, 5/5	+, 5/5	+, 2/5	ND	ND	+, 4/5	+, 4/5
Zhang et al[4]	LG-FLAC	+, 3/3	C/N+, 3/3	+, 0/3	−, 0/3	ND	ND	+, 3/3	+, 3/3
Suzuki et al[19]	HG-FLAC	+, 33/52	M+	ND	+, 20/52	+, 9/52	+, 19/52	ND	ND
Zhang et al[20]	LG-FLAC	+, 11/13	M+, 10/10	+, 4/7	+, 2/8	ND	ND	+, 17/26	+, 11/15

C/N indicates cytoplasmic/nuclear staining; Gly-3, glypican-3; M, membranous staining; ND, no description; TTF-1, thyroid transcription factor-1.

Copyright © 2021 The Author(s). Published by Wolters Kluwer Health, Inc.

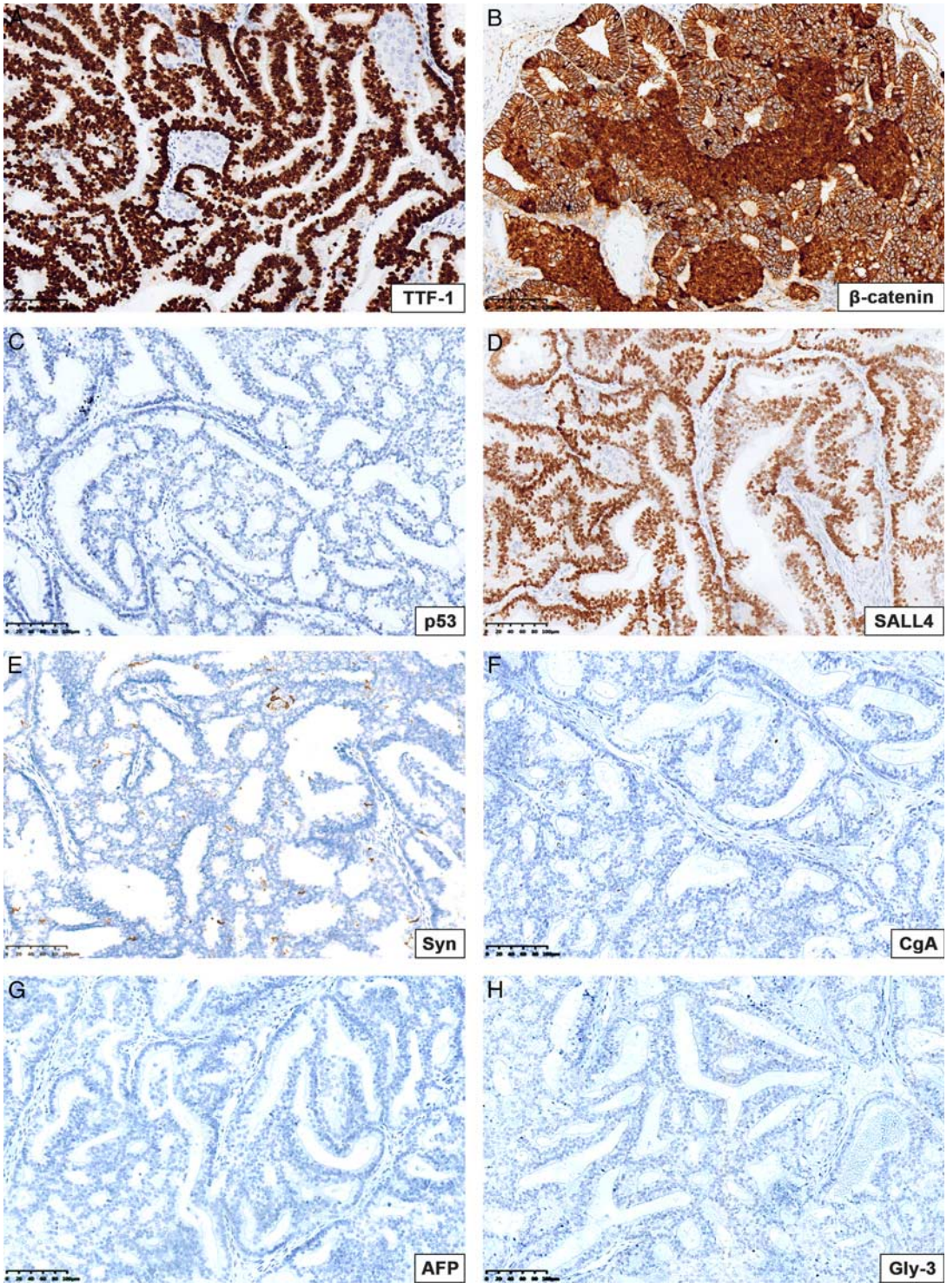

FIGURE 3. IHC characteristics of LG-FLAC. A, Diffuse positive staining for thyroid transcription factor-1. B, Nuclear/cytoplasmic staining pattern for β-catenin. C, Total absence of staining for p53. D, Moderately positive staining of partial glands for SALL-4. E, Moderate staining for Syn in about 1% LG-FLAC cells. F–H, Absence of staining for CgA (F), APF (G), and Gly-3 (H) in LG-FLAC. Gly-3 indicates glypican-3.

site mutation (c.5096-1G > T) and 1 missense mutation (D1810Y) of *DICER1* were detected in case LG4. Moreover, a novel missense mutation *MYCN* P44L, which has not been previously reported in FLAC, was detected in the 2 LG-FLAC cases (Fig. 5A; Table S1, Supplemental Digital Content 4, http://links.lww.com/PAS/B188).

Copyright © 2021 The Author(s). Published by Wolters Kluwer Health, Inc.

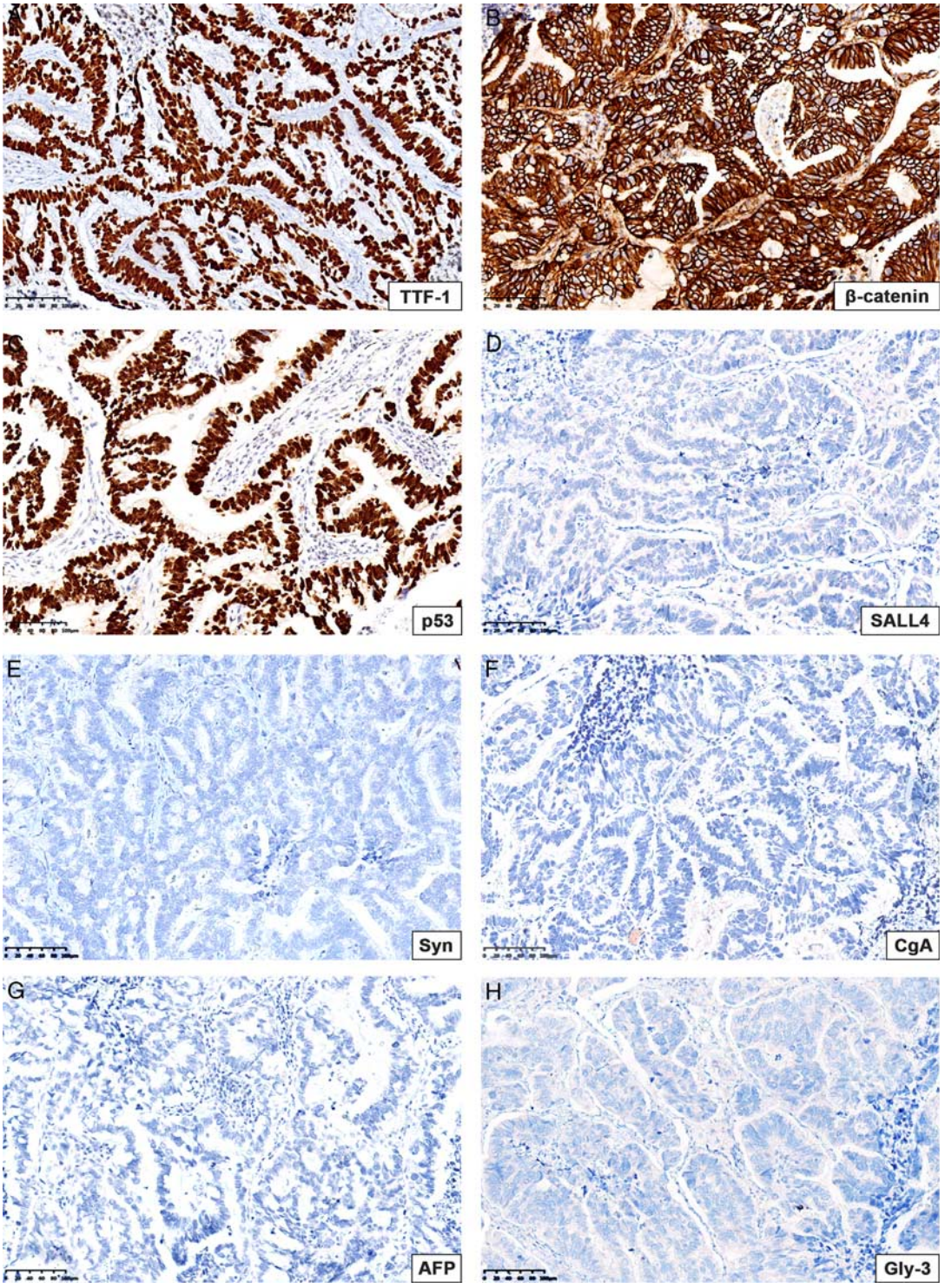

FIGURE 4. IHC features of HG-FLAC. A, Strong positive pattern of staining for thyroid transcription factor-1. B, Membranous pattern of staining for β-catenin. C, Strong and diffuse pattern of staining for p53. D–H, HG-FLAC samples were virtually negative for SALL-4 (D), Syn (E), CgA (F), APF (G), or Gly-3 (H). Gly-3 indicates glypican-3.

TSC2 nonsense mutation R1032* was found in case LG1, and *EGFR* mutation D247G in exon 6 was detected in case LG2. Notably, the latter mutation was not located in the *EGFR* hot mutation zone in exons 18 to 21. We also noticed copy number gains of *HER2* (4.8 copies) and *SOX9* (6.8 copies) in case LG2, and we further confirmed the true amplification status of *HER2* by fluorescence in situ hybridization (Fig. 5B). SOX9 is not only a

Copyright © 2021 The Author(s). Published by Wolters Kluwer Health, Inc.

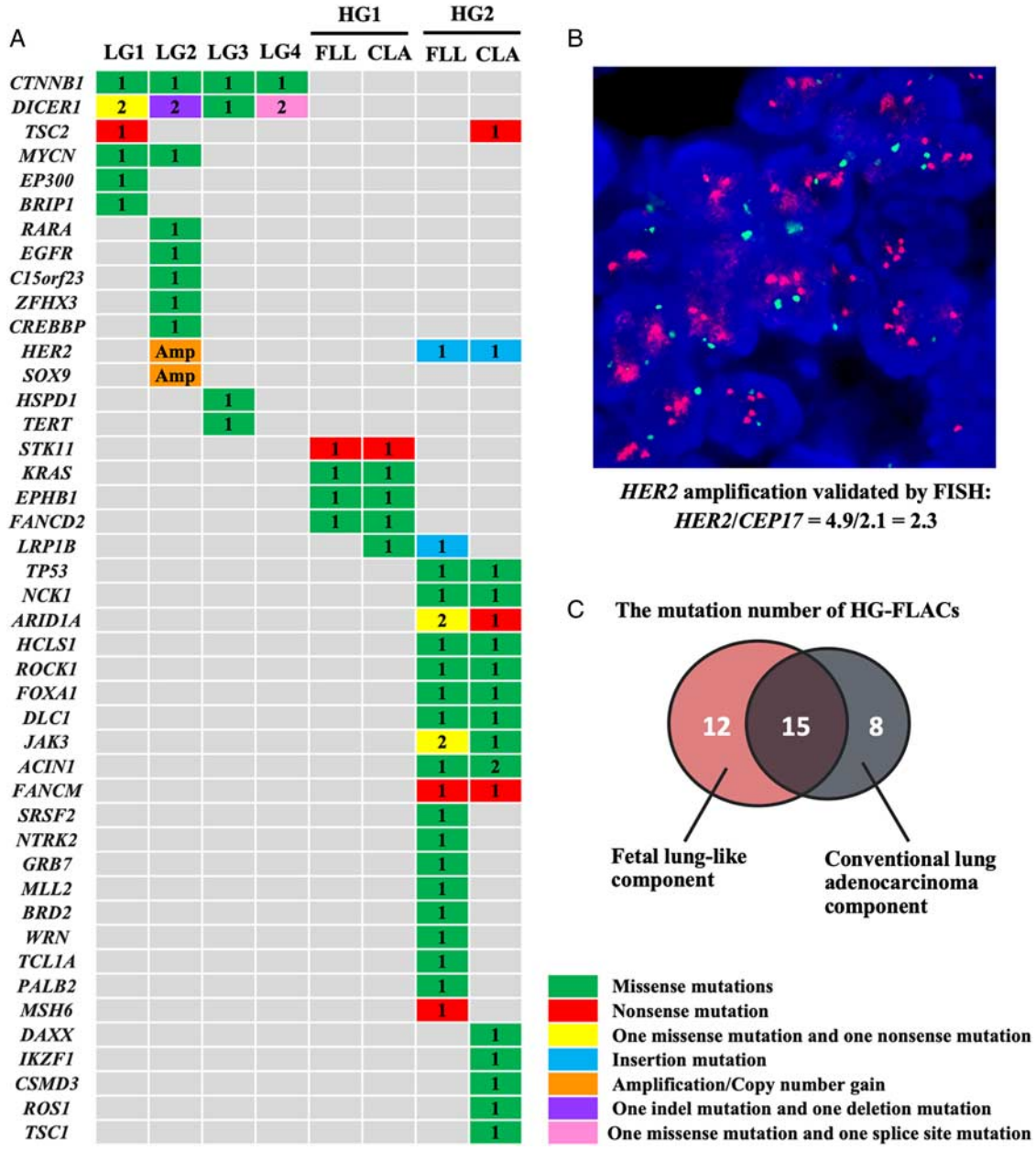

FIGURE 5. Molecular analysis of LG-FLAC and HG-FLAC by NGS. A, The types and numbers of genetic variations in 4 cases of LG-FLAC (LG1-4) and 2 cases of HG-FLAC (HG1-2) determined by NGS based on the 1021-gene panel. B, More than 2-fold higher number of *HER2* signals than of *CEP17* signals was observed according to the fluorescence in situ hybridization, which confirmed the *HER2* amplification result of NGS. C, Venn diagram illustrating the number of mutations of the FLL and CLA components in the 2 cases of HG-FLAC: 15 of 35 mutations were detected in both components of HG-FLAC samples.

progenitor marker but is also required for normal progenitor branching in the early development of the lung.[21] However, the *SOX9* amplification status could not be validated by fluorescence in situ hybridization due to the lack of a specific probe.

To determine the molecular spectra of the FLL and CLA components of HG-FLAC, DNA samples of the 2 distinct morphologic components were separately isolated and sequenced. The mutational profiles of the 2 HG-FLAC components largely overlapped (Figs. 5A, C; Table S2, Supplemental Digital Content 5, http://links.lww.com/PAS/B189). Case HG1 harbored mutations of *STK11* (E199*), *KRAS* (G13C), *EPHB1* (T123S), and *FANCD2* (R328L) in both components, whereas 1 mutation, *LRP1B* M681R, was exclusively found in the CLA component (Table 5). In case HG2, there were 11 mutations in both the FLL and CLA components, among which a missense mutation in *TP53* (R273C) and an insertion mutation in *HER2* (A775_G776insYVMA) were particularly noteworthy, because they have been considered as 2 hotspots in

Copyright © 2021 The Author(s). Published by Wolters Kluwer Health, Inc.

TABLE 4. Characteristic Molecular Mutations LG-FLAC and HG-FLAC Cases in the Present Study and Literature Review

References	Diagnosis	CTNNB1	DICER1	MYCN	Other Genes
This study	LG-FLAC	p.S33C	p.Q488* p.D1709V	p.P44L	
This study	LG-FLAC	p.S37F	p.D1810F p.A1710del	p.P44L	
This study	LG-FLAC	p.D32Y	p.D1709A		
This study	LG-FLAC	p.S37F	c.5096-1G > T p.D1810Y		
Nakatani et al[22]	LG-FLAC	p.G34V p.S37C			
Sekine et al[23]	LG-FLAC	p.A32T p.S37C p.S33C			
Wu et al[9]	LG-FLAC		p.T1180*		
De Kock et al[24]	LG-FLAC	p.S33C	p.A1709G		
Fu et al[8]	LG-FLAC	p.S37Y p.S37C			
Liu et al[25]	LG-FLAC	p.S33C	p.D1709N p.S1470L*fs19		
This study	HG-FLAC				*STK11* p.E199*, *KRAS* p.G13C
This study	HG-FLAC				*TP53* p.R273C, *ERBB2* p.A775_G776insYVMA
Morita et al[7]	HG-FLAC				*KRAS* Codon 12/13, *EGFR* L858R
Suzuki et al[18]	HG-FLAC				*EGFR* L858R, E746_A750del, *PIK3CA* E545A
Zhang et al[4]	HG-FLAC				*EGFR* L858R, T790M

*Termination codon.

NSCLC and detected at high frequencies in HG2. In total, 15 of 28 mutations were simultaneously detected in both the FLL and CLA components of the 2 HG-FLAC cases, and the frequencies of these mutations in both components were quite close. The recurrent mutations of *CTNNB1* and *DICER1* categorized by the original studies and by the genetic locus are separately summarized in Table 4 and Figure S2 (Supplemental Digital Content 1, http://links.lww.com/PAS/B185).

Treatment and Survival

The 3 patients with early-stage LG-FLAC underwent lobectomy or pneumonectomy together with mediastinal lymphadenectomy. Among these patients, only patient LG2 was treated by adjuvant chemotherapy. Because patient LG4 had developed multifocal metastasis of bones at diagnosis, she could not undergo a surgical treatment and therefore received palliative chemotherapy. All LG-FLAC patients were regularly examined to monitor relapse, and they were all alive until the last follow-up. Patient HG1 received pemetrexed plus nedaplatin adjuvant after a radical resection of the tumor located in the middle lobe of the right lung, and he was alive without recurrence until the last follow-up. Patient HG2 had received pemetrexed, carboplatin, and bevacizumab as neoadjuvant therapy before the surgery and palliative chemotherapy thereafter. In light of the NGS results (*HER2* A775_G776insYVMA), the patient accepted afatinib treatment, but his brain metastasis still progressed 3.7 months later, and he died at 13.7 months after the disease diagnosis (Table 2).

TABLE 5. Comparison of the Clinical Features of LG-FLAC and HG-FLAC Cases From Retrieved Literatures and the Present Study

	LG-FLAC	HG-FLAC	*P*
Total cases	77	97	—
Age, mean	35.7 (6-72)	64.6 (51-85)	< 0.001
Sex			
Male	38	79	< 0.001
Female	39	18	
TNM stage			0.0022
I/II	58	70	
III/IV	5	27	
No description	14	0	
Smoking status			< 0.001
Yes	16	72	
No	14	15	
No description	47	10	
5 y OS rate (%)	66.7-100.0	40.0-82.4	—

Differences Between LG-FLAC and HG-FLAC According to Published Reports

After a careful review, 12 articles with featured molecular findings[4,7–9,18,22–25] and/or detailed clinicopathologic, IHC description[4,7,17–20] were included and summarized in Tables 2–4. Clinical features of 77 LG-FLAC and 97 HG-FLAC cases from the published studies and the current study were analyzed (Table 5). The patients with LG-FLAC were significantly younger than those with HG-FLAC (mean ages, 35.7 and 64.6 y, $P < 0.001$). There was a predominance of males in HG-FLAC, with a male-to-female ratio of 4.4:1. The patients

Copyright © 2021 The Author(s). Published by Wolters Kluwer Health, Inc.

with HG-FLAC were more frequently diagnosed at stages III/IV than the ones with LG-FLAC ($P = 0.0022$). Most patients with HG-FLAC were smokers, whereas only a low proportion of patients with LG-FLAC had a history of smoking ($P < 0.001$). With regards to the prognosis, the 5-year OS rate of patients with LG-FLAC was generally higher than that of HG-FLAC (66.7% to 100.0% and 40.0% to 82.4%, respectively).

DISCUSSION

In this study, we performed a comprehensive analysis of the clinicopathologic, IHC, and genetic features of LG-FLAC and HG-FLAC cases, and compared the genetic profiles of the FLL and CLA components of HG-FLAC by NGS. Patients with HG-FLAC were elderly male smokers at advanced TNM stages, whereas most patients with LG-FLAC tended to be much younger and at an early TNM stage. The typical morphologic and IHC features of LG-FLAC and HG-FLAC were in agreement with previous reports.[4,6–8] However, in addition to the frequent mutations in genes, such as *CTNNB1* and *DICER1* in LG-FLAC, we uncovered the missense *MYCN* mutation P44L in 2 LG-FLACs samples, which has not been linked to LG-FLAC before. Therefore, it could be used as a molecular marker in auxiliary LG-FLAC diagnosis. The absence of *CTNNB1*, *DICER1*, or *MYCN* mutations in the FLL component of HG-FLAC indicated that HG-FLAC is different from LG-FLAC. The high proportion of mutations detected in HG-FLAC samples coexisted in both FLL and CLA components, indicating that these 2 distinct morphologic elements were more similar genetically than could be assumed based on previous studies. Mutations commonly observed in CLA, such as *STK11*/*KRAS* comutation,[26] *TP53* missense mutation,[27] and *HER2* insertion mutation,[28] have been detected in both components of HG-FLACs, demonstrating that this cancer more likely represents a special morphologically distinct subtype of CLA.

Aberrant β-catenin nuclear/cytoplasmic staining pattern has been considered as a hallmark of LG-FLAC.[1,7] Another valuable IHC marker is p53, which is expressed strongly in HG-FLAC, but is nearly absent in LG-FLAC. It had been shown that ~80% of HG-FLACs display IHC evidence of neuroendocrine differentiation.[7] However, HG-FLAC samples were negative for CgA and Syn in the current study, and LG-FLAC samples were only focally positive for Syn, indicating that the neuroendocrine differentiation tendency is not always present in FLAC. Staining for AFP had been observed in 29% to 47% of HG-FLACs,[4,7] but, in this study, both HG-FLAC and LG-FLAC samples were negative for AFP. Given that the positive grade of the neuroendocrine and embryonic markers is dependent on the existence and proportion of the corresponding component, the absence of corresponding positive staining in FLAC may not be used as an informative indicator.

CTNNB1 mutations are a typical genetic alteration in LG-FLAC. Classically, *CTNNB1* exon 3 mutations are associated with decreased degradation of β-catenin, accumulation of β-catenin protein in the cytoplasm, and its subsequent translocation to the nucleus,[23] which reasonably explain the immunophenotypic feature of β-catenin staining in LG-FLAC. *CTNNB1* encodes a key protein necessary for the maintenance of lung epithelial progenitors after their foregut specification; human embryonic stem cell-derived lung progenitors also depend on CTNNB1-mediated Wnt signaling to suppress the gastrointestinal fate.[29] Therefore, Wnt-activating mutations of *CTNNB1* that lead to the abnormal induction and/or continued progenitor proliferation might be the intrinsic drivers of LG-FLAC. Previously, the *TSC2* F408V mutation was detected in LG-FLAC (mutation frequency 52.8%) by NGS targeting a 56-gene panel.[8] In the current study, another *TSC2* mutation (R1032*, 2.7%) was identified in one LG-FLAC sample (Table S1). The *de novo* defects in *TSC1/2* are considered as the main cause and a diagnostic molecular marker of tuberous sclerosis.[30] It has been hypothesized that *TSC2* mutations abolish the ability of this protein to inhibit Wnt-stimulated β-catenin-dependent transcription,[31,32] suggesting that *TSC2* and *CTNNB1* mutations could be synergistic in activating the Wnt/β-catenin pathway in LG-FLAC. However, *CTNNB1* mutations are relatively broad-spectrum across many cancer types, rendering the coexistence with less common mutations in *DICER1* and *MYCN* more indicative and specific for LG-FLAC diagnosis.

DICER1 encodes an endoribonuclease from the RNase III family that plays an essential role in microRNA production.[33] Germline inactivation *DICER1* is associated with the familial *DICER1* syndrome.[34] Classic *DICER1*-associated tumors include pleuropulmonary blastoma,[35] Wilms tumor,[36] Sertoli-Leydig cell tumor,[37] uterine cervical embryonal rhabdomyosarcoma,[38] multinodular goiter,[39] nasal chondromesenchymal hamartoma,[40] and others. A 16-year-old Chinese *DICER1* mutation (Tyr1180*) carrier reportedly presented with LG-FLAC, Sertoli-Leydig cell ovarian tumor, and familial multinodular goiter.[9] Similarly, *DICER1* mutations were present in all the 4 LG-FLAC cases in the present study, indicating that LG-FLAC may be one of the diverse manifestations of the *DICER1* syndrome, and *DICER1* mutations could serve as a valuable diagnostic molecular marker for LG-FLAC.

In addition to *CTNNB1* and *DICER1* mutations frequently reported in previous studies, numerous novel mutations were also identified in our study. One important discovery was *MYCN* P44L, which was found in 2 different patients with LG-FLAC. *MYCN* P44L was predicted to be harmful by SIFT and PolyPhen-2, and it has been recorded in the Catalog of Somatic Mutations in the Cancer Database (https://cancer.sanger.ac.uk/cosmic) and in the cBioPortal for Cancer Genomics (http://cbioportal.org/msk-impact). Moreover, *MYCN* P44L has been reported in neuroblastoma,[41] basal cell carcinoma,[42] and Wilms tumor[43] as an acquired somatic variant with a presumed gain of function. The specific role of the *MYCN* P44L mutation in malignancies of the lung remains unclear, which warrants further research in this field.

Copyright © 2021 The Author(s). Published by Wolters Kluwer Health, Inc.

Some classic oncogenic mutations commonly observed in CLA were concurrently recognized in both the FLL and CLA components of HG-FLACs in our study. *STK11* (or *LKB1*) is among the most frequently inactivated tumor-suppressor genes, often comutated with *KRAS* in NSCLC[44]; patients with mutations in both *STK11* and *KRAS* had a significantly lower objective response rate to PD-1 blockade and a shorter OS than in patients with *KRAS* mutations only.[45] A775_G776insYVMA is the most common type of *HER2* exon 20 insertions; this specific mutation often co-occurs with *TP*53 mutations and is associated with inferior response to afatinib in NSCLC,[46] which may explain the fast exacerbation of the brain lesion following treatment with afatinib in case HG2. *ARID1A* is a subunit of the SWI/SNF chromatin remodeler that influences the accessibility of proteins to DNA,[47] and *ARID1A* mutations have been found in 8% to 12% of NSCLC cases.[48] The simultaneous existence of the above gene variations in both components strongly supports the notion that HG-FLAC genetically resembles conventional NSCLC.

In this study, we applied multiple experimental techniques to comprehensively determine the clinicopathologic, IHC, and genetic features of LG-FLAC and HG-FLAC. The macrodissection step made it possible to separately analyze molecular profiles of different components of HG-FLAC. The NGS panel was much larger than previously used panels, and the comparison of the mutational spectra of LG-FLAC and HG-FLAC suggests that HG-FLAC is quite different from LG-FLAC, with more resemblance to CLA, from the genetic standpoint. Admittedly, this study has several limitations that should be acknowledged. The actual biological function of the novel mutation *MYCN* P44L in LG-FLAC cases was not explored experimentally, and we believe that this mutational marker warrants a deeper investigation in future studies. The number of included cases was very small owing to the rarity of the disease itself, so we additionally reviewed 12 published reports and integrated the clinicopathologic, IHC, and molecular results with the cases in the current study, to better demonstrate the differences between LG-FLAC and HG-FLAC.

In conclusion, in addition to morphologic and IHC differences, mutations of *CTNNB1*, *DICER1*, and *MYCN* can serve as specific diagnostic molecular markers for LG-FLAC. HG-FLAC is quite different from LG-FLAC in clinicopathologic, IHC, and genetic aspects; therefore, it should be treated as a subtype of CLA rather than a variation of FLAC.

REFERENCES

1. Ricaurte LM, Arrieta O, Zatarain-Barrón ZL, et al. Comprehensive review of fetal adenocarcinoma of the lung. *Lung Cancer (Auckl)*. 2018;9:57–63.
2. Kradin RL, Young RH, Dickersin GR, et al. Pulmonary blastoma with argyrophil cells and lacking sarcomatous features (pulmonary endodermal tumor resembling fetal lung). *Am J Surg Pathol*. 1982;6:165–172.
3. Kodama T, Shimosato Y, Watanabe S, et al. Six cases of well-differentiated adenocarcinoma simulating fetal lung tubules in pseudoglandular stage. *Am J Surg Pathol*. 1984;8:735–744.
4. Zhang J, Sun J, Liang XL, et al. Differences between low and high grade fetal adenocarcinoma of the lung: a clinicopathological and molecular study. *J Thorac Dis*. 2017;9:2071–2078.
5. Travis WD, Brambilla E, Nicholson AG, et al. The 2015 World Health Organization Classification of Lung Tumors. *J Thorac Oncol*. 2015;10:1243–1260.
6. Nakatani Y, Kitamura H, Inayama Y, et al. Pulmonary adenocarcinomas of the fetal lung type: a clinicopathologic study indicating differences in histology, epidemiology, and natural history of low-grade and high-grade forms. *Am J Surg Pathol*. 1998;22:399–411.
7. Morita S, Yoshida A, Goto A, et al. High-grade lung adenocarcinoma with fetal lung–like morphology: clinicopathologic, immunohistochemical, and molecular analyses of 17 cases. *Am J Surg Pathol*. 2013;37:924–932.
8. Fu Y, Wu Q, Su F, et al. Novel gene mutations in well-differentiated fetal adenocarcinoma of the lung in the next generation sequencing era. *Lung Cancer*. 2018;124:1–5.
9. Wu Y, Chen D, Li Y, et al. DICER1 mutations in a patient with an ovarian Sertoli-Leydig tumor, well-differentiated fetal adenocarcinoma of the lung, and familial multinodular goiter. *Eur J Med Genet*. 2014;57:621–625.
10. Sun P, Zhong Z, Lu Q, et al. Mucinous carcinoma with micropapillary features is morphologically, clinically and genetically distinct from pure mucinous carcinoma of breast. *Mod Pathol*. 2020;33:1945–1960.
11. Wang J, Yi Y, Xiao Y, et al. Prevalence of recurrent oncogenic fusion in mismatch repair-deficient colorectal carcinoma with hypermethylated MLH1 and wild-type BRAF and KRAS. *Mod Pathol*. 2019;32:1053–1064.
12. Zhang Y, Chang L, Yang Y, et al. The correlations of tumor mutational burden among single-region tissue, multi-region tissues and blood in non-small cell lung cancer. *J Immunother Cancer*. 2019;7:98.
13. Li H, Durbin R. Fast and accurate short read alignment with Burrows-Wheeler transform. *Bioinformatics*. 2009;25:1754–1760.
14. Cibulskis K, Lawrence MS, Carter SL, et al. Sensitive detection of somatic point mutations in impure and heterogeneous cancer samples. *Nat Biotechnol*. 2013;31:213–219.
15. Wang K, Li M, Hakonarson H. ANNOVAR: functional annotation of genetic variants from high-throughput sequencing data. *Nucleic Acids Res*. 2010;38:e164–e164.
16. Li J, Lupat R, Amarasinghe KC, et al. CONTRA: copy number analysis for targeted resequencing. *Bioinformatics*. 2012;28:1307–1313.
17. Sato S, Koike T, Yamato Y, et al. Resected well-differentiated fetal pulmonary adenocarcinoma and summary of 25 cases reported in Japan. Japanese. *J Thorac Cardiovasc Surg*. 2006;54:539–542.
18. Suzuki M, Yazawa T, Ota S, et al. High-grade fetal adenocarcinoma of the lung is a tumour with a fetal phenotype that shows diverse differentiation, including high-grade neuroendocrine carcinoma: a clinicopathological, immunohistochemical and mutational study of 20 cases. *Histopathology*. 2015;67:806–816.
19. Suzuki M, Nakatani Y, Ito H, et al. Pulmonary adenocarcinoma with high-grade fetal adenocarcinoma component has a poor prognosis, comparable to that of micropapillary adenocarcinoma. *Mod Pathol*. 2018;31:1404–1417.
20. Zhang TM, Lu BH, Cai YR, et al. Well-differentiated fetal adenocarcinoma of the lung: clinicopathologic features of 45 cases in China. *Int J Clin Exp Pathol*. 2018;11:1587–1598.
21. Rockich BE, Hrycaj SM, Shih HP, et al. Sox9 plays multiple roles in the lung epithelium during branching morphogenesis. *Proc Natl Acad Sci USA*. 2013;110:E4456–E4464.
22. Nakatani Y, Masudo K, Inayama Y, et al. Aberrant nuclear localization and gene mutation of β-catenin in low-grade adenocarcinoma of fetal lung type: Up-regulation of the Wnt signaling pathway may be a common denominator for the development of tumors that form morules. *Mod Pathol*. 2002;15:617–624.
23. Sekine S, Shibata T, Matsuno Y, et al. β-Catenin mutations in pulmonary blastomas: association with morule formation. *J Pathol*. 2003;200:214–221.
24. De Kock L, Bah I, Wu Y, et al. Germline and somatic DICER1 mutations in a well-differentiated fetal adenocarcinoma of the lung. *J Thorac Oncol*. 2016;11:e31–e33.
25. Liu S, Wang J, Luo X, et al. Coexistence of low-grade fetal adenocarcinoma and adenocarcinoma in situ of the lung harboring

Copyright © 2021 The Author(s). Published by Wolters Kluwer Health, Inc.

different genetic mutations: a case report and review of literature. *Onco Targets Ther*. 2020;13:6675–6680.
26. Skoulidis F, Byers LA, Diao L, et al. Co-occurring genomic alterations define major subsets of KRAS-mutant lung adenocarcinoma with distinct biology, immune profiles, and therapeutic vulnerabilities. *Cancer Discov*. 2015;5:860–877.
27. Cai X, Chen Z, Deng M, et al. Unique genomic features and prognostic value of COSMIC mutational signature 4 in lung adenocarcinoma and lung squamous cell carcinoma. *Ann Transl Med*. 2020;8:1176.
28. Collisson EA, Campbell JD, Brooks AN, et al. Comprehensive molecular profiling of lung adenocarcinoma. *Nature*. 2014;511:543–550.
29. Ostrin EJ, Little DR, Gerner-Mauro KN, et al. β-Catenin maintains lung epithelial progenitors after lung specification. *Development*. 2018;145:dev160788.
30. Suspitsin EN, Yanus GA, Dorofeeva MY, et al. Pattern of TSC1 and TSC2 germline mutations in Russian patients with tuberous sclerosis. *J Hum Genet*. 2018;63:597–604.
31. Jozwiak J, Wlodarski P. Hamartin and tuberin modulate gene transcription via β-catenin. *J Neurooncol*. 2006;79:229–234.
32. Jozwiak J, Kotulska K, Grajkowska W, et al. Upregulation of the WNT pathway in tuberous sclerosis-associated subependymal giant cell astrocytomas. *Brain Dev*. 2007;29:273–280.
33. Ryan BM, Robles AI, Harris CC. Genetic variation in microRNA networks: the implications for cancer research. *Nat Rev Cancer*. 2010;10:389–402.
34. Kamihara J, Paulson V, Breen MA, et al. DICER1-associated central nervous system sarcoma in children: comprehensive clinicopathologic and genetic analysis of a newly described rare tumor. *Mod Pathol*. 2020;33:1910–1921.
35. Pugh TJ, Yu W, Yang J, et al. Exome sequencing of pleuropulmonary blastoma reveals frequent biallelic loss of TP53 and two hits in DICER1 resulting in retention of 5p-derived miRNA hairpin loop sequences. *Oncogene*. 2014;33:5295–5302.
36. Gadd S, Huff V, Walz AL, et al. A Children's Oncology Group and TARGET initiative exploring the genetic landscape of Wilms tumor. *Nat Genet*. 2017;49:1487–1494.
37. Rio Frio T, Bahubeshi A, Kanellopoulou C, et al. DICER1 mutations in familial multinodular goiter with and without ovarian Sertoli-Leydig cell tumors. *JAMA*. 2011;305:68–77.
38. Tomiak E, de Kock L, Grynspan D, et al. DICER1 mutations in an adolescent with cervical embryonal rhabdomyosarcoma (cERMS). *Pediatr Blood Cancer*. 2014;61:568–569.
39. Rath SR, Bartley A, Charles A, et al. Multinodular goiter in children: an important pointer to a germline DICER1 mutation. *J Clin Endocrinol Metab*. 2014;99:1947–1948.
40. Stewart DR, Messinger Y, Williams GM, et al. Nasal chondromesenchymal hamartomas arise secondary to germline and somatic mutations of DICER1 in the pleuropulmonary blastoma tumor predisposition disorder. *Hum Genet*. 2014;133:1443–1450.
41. Pugh TJ, Morozova O, Attiyeh EF, et al. The genetic landscape of high-risk neuroblastoma. *Nat Genet*. 2013;45:279–284.
42. Bonilla X, Parmentier L, King B, et al. Genomic analysis identifies new drivers and progression pathways in skin basal cell carcinoma. *Nat Genet*. 2016;48:398–406.
43. Williams RD, Chagtai T, Alcaide-German M, et al. Multiple mechanisms of MYCN dysregulation in Wilms tumour. *Oncotarget*. 2015;6:7232–7243.
44. Facchinetti F, Bluthgen MV, Tergemina-Clain G, et al. LKB1/STK11 mutations in non-small cell lung cancer patients: descriptive analysis and prognostic value. *Lung Cancer*. 2017;112:62–68.
45. Skoulidis F, Goldberg ME, Greenawalt DM, et al. STK11/LKB1 mutations and PD-1 inhibitor resistance in KRAS-mutant lung adenocarcinoma. *Cancer Discov*. 2018;8:822–835.
46. Fang W, Zhao S, Liang Y, et al. Mutation variants and co-mutations as genomic modifiers of response to afatinib in HER2-mutant lung adenocarcinoma. *Oncologist*. 2020;25:e545–e554.
47. Wu RC, Wang TL, Shih IM. The emerging roles of ARID1A in tumor suppression. *Cancer Biol Ther*. 2014;15:655–664.
48. Karachaliou N, Paulina Bracht JW, Rosell R. ARID1A gene driver mutations in lung adenocarcinomas. *J Thorac Oncol*. 2018;13:e255–e257.

Copyright © 2021 The Author(s). Published by Wolters Kluwer Health, Inc.